Geothermics 53 (2015) 125–132

Contents lists available at ScienceDirect

Geothermics

journal homepage: www.elsevier.com/locate/geothermics

Fractional derivative-based tracer analysis method for the characterization of mass transport in fractured geothermal reservoirs

Anna Suzuki[a,*], Yuichi Niibori[b], Sergei A. Fomin[c], Vladimir A. Chugunov[d], Toshiyuki Hashida[e]

[a] Graduate School of Environmental Studies, Tohoku University, Sendai 980-8579, Japan
[b] Graduate School of Engineering, Tohoku University, Sendai 980-8579, Japan
[c] Department of Mathematics and Statistics, California State University, Chico, CA 95929, USA
[d] Department of Applied Mathematics, Kazan Federal University, Kazan 420008, Russia
[e] Fracture and Reliability Research Institute, Tohoku University, Sendai 980-8579, Japan

ARTICLE INFO

Article history:
Received 29 April 2013
Accepted 9 May 2014

Keywords:
Fractional advection-dispersion
Fractal geometry
Mass transport
Fractured reservoir
Geothermal resources
Reinjection

ABSTRACT

The fractional advection-dispersion equation (fADE) has been proposed to describe mass transport in a fractured reservoir. This study develops a finite discrete method to solve the fADE and tests its accuracy against analytical solutions. Tracer simulation uses a three-dimensional simulation of flow analysis (FRACSIM-3D). The solution to the fADE incorporating a spatial fractional derivative shows reasonable agreement with the tracer response from FRACSIM-3D, which shows highly anomalous behaviors such as a long tail. The prediction by the fADE model is reasonably similar to those of FRACSIM-3D irrespective of differing well intervals.

1. Introduction

The lifespan of geothermal resources may be prolonged by a reinjection process, thereby delaying pressure decline and preventing run-out of water in a geothermal reservoir (Stefansson, 1997; Kaya et al., 2011; Axelsson et al., 2005). However, one of the important problems with reinjection is the possibility of an early thermal breakthrough in production wells. Premature breakthrough and injection-induced cooling continue to be problems associated with injection into the geothermal reservoir. Evaluation of the effect of injected water on flow and thermal properties within the geothermal reservoir is essential for the optimal management and protection of subsurface fluid resources.

Tracer testing is a standard method of determining mass transport within a geothermal reservoir and can be a valuable tool in the design and management of production and injection operations (Horne, 1985; Niibori et al., 1995; Pruess, 2002). Methods have also been discussed for predicting thermal breakthrough in fractured reservoirs based on information from tracer tests, e.g., by Lauwerier (1955), Gringarten et al. (1975), Gringarten and Sauty (1975), Pruess and Bodvarsson (1984), and Kocabas (2005). Shook (2001) discussed the potential application of tracer data to provide relatively simple reservoir properties and to predict thermal breakthrough. Such information could provide a means of optimizing injection conditions and managing energy extraction (Wu et al., 2008). Furthermore, Lovekin and Horne (1989) and Juliusson and Horne (2013) reported methods for optimizing injection schedules in geothermal reservoirs based on tracer return data using numerical simulations. In these cases, the production and injection wells were supposed to be already installed. The proposed method can be advantageous to predict mass transport at a location without any wells; and, based on field tracer data obtained from a limited number of wells, to determine where to optimally locate injection and/or production wells.

The inter-well properties provided by tracer tests are strongly controlled by the fracture geometries. Flow simulation models based on geological observation are often used to attempt quantitative assessment of tracer response curves. Discrete and continuum approaches form the two main branches in modeling the fluid flow and solute transport in fractured rocks. Simulations using the discrete fracture system or the hybrid discrete continuum system with hundreds or thousands of fractures were developed from a

* Corresponding author at: Graduate School of Environmental Studies, Tohoku University, 6-6-11-707, Aramaki Aza Aoba, Aoba, Sendai, Miyagi 980-8579, Japan. Tel.: +81 22 795 7524; fax: +81 22 795 4311.
E-mail address: anna.suzuki@rift.mech.tohoku.ac.jp (A. Suzuki).

http://dx.doi.org/10.1016/j.geothermics.2014.05.003
0375-6505/

need to represent more realistic fracture system geometries (Long and Witherspoon, 1985; Zimmerman and Bodvarsson, 1996). Since the discrete fracture network models incorporate many details and data, understanding and quantifying the geological and physical uncertainties remains the main task for the development of such models (Neuman, 2005). Numerical simulations used commonly in the previous studies depict the rock as a dual continuum, and include the dual porosity method (Barenblatt et al., 1960; Coats and Smith, 1964), dual permeability method (Gerke and van Genuchten, 1993), and the more general multi-interacting continua (MINC) method (Warren and Root, 1963; Kazemi, 1969; Pruess and Narasimhan, 1985). The continuum approaches can be managed to simulate the flow and mass transport in a fractured reservoir using relatively few parameters compared with the discrete fracture approach. Nevertheless, in order to characterize complicated structures, a simulation model is required to incorporate many input parameters, and thus model calibration requires either time-consuming statistical treatment or subjective evaluation.

A classical transport model, which can be used to analyze the tracer experiments, is the one-dimensional form of the well-known advection-dispersion equation (ADE) (Bear, 1972):

$$\frac{\partial c}{\partial t} = -u\frac{\partial c}{\partial x} + D\frac{\partial^2 c}{\partial x^2} \tag{1}$$

Here, c is solute concentration, u the average linear velocity, x the distance, τ the time, and D [m^2/s] is the dispersion coefficient. This model describes mass transport in the standard continuum description using the macroscale mass transport variables such as velocity and dispersion coefficient.

In many field experiments effluent tracer breakthrough curves often display a persistent skewness or leading and/or trailing edges that cannot be explained by the ADE. Some researches suggest that long tailings are attributed to recycling of the tracer, or injection conditions (Rose et al., 2004; Juliusson and Horne, 2013). However, non-Fickian tails have also been observed on a simple experiment conditions in laboratory-scale and field-scale tracer tests (Hatano and Hatano, 1998). Complexity of fracture distribution in a reservoir has been discussed to interpret the observed tailings in previous studies. Mathematical models accounting for diffusion and interaction of solutes with the intact rock matrix (Neretnieks, 1983; Moreno et al., 1985), discrete flow channeling (Neretnieks et al., 1982; Tsang and Tsang, 1987), and fracture-matrix model (Bullivant and O'Sullivan, 1989) have been proposed. A generalization of the mobile/immobile phase transport equation was given by the fractional advection-dispersion equation (fADE) (Benson et al., 2000a, 2000b; Schumer et al., 2003; Zhang et al., 2009). Fomin et al. (2011), amongst others, focused on the effects of fracture (fractal) geometry in a fractured reservoir on mass transport and derived the fADE through the use of fractional derivatives in time and space. Understanding of the complex fracture pattern in geothermal reservoirs is of crucial importance for the design of reinjections. The fADE can provide anomalous behaviors of tracer responses using limited parameters, which makes it possible to quickly and efficiently analyze mass transport in a fractured reservoir.

In this study, we discuss the applicability of the fADE derived by Fomin et al. (2011). Recently, we reported that the fADE (Fomin et al., 2011) showed good agreement with tracer responses including tailings, which were simulated by a numerical simulation of fractured reservoirs. The tracer test was performed during reinjection operation, namely in the case where water is introduced at an injection well and reaches a production well at atmospheric pressure. In that case, the prediction was verified for confined well spacing (50–80 m). The objective of this paper is to extend the tracer analysis of Suzuki et al. (2012). This paper presents tracer tests performed in one-dimensional flow as natural condition, and fADE was applied for prediction at wider well spacing (~500 m).

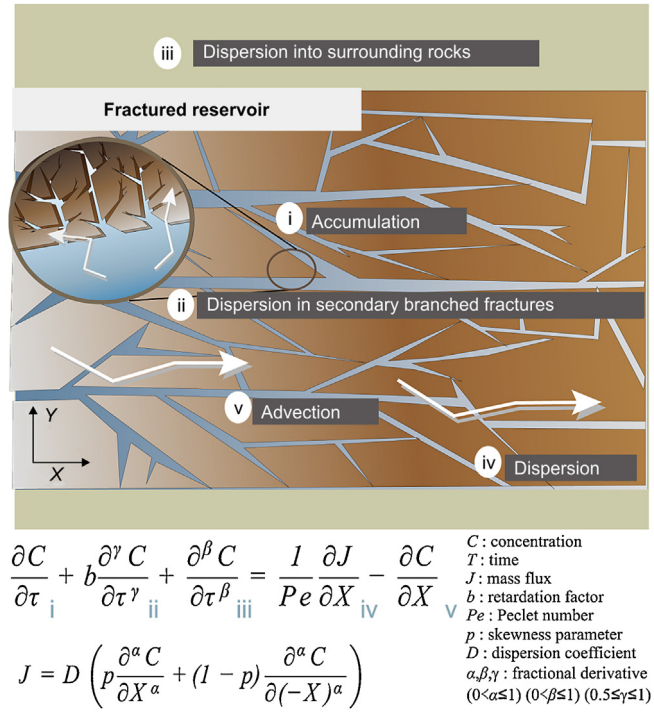

Fig. 1. Schematic of the fADE in a fractured aquifer.

2. Mathematical model of mass transport

2.1. Governing equation

Fomin et al. (2011) proposed the one-dimensional fractional advection-dispersion equation (fADE) to model solute transport in a fracture (fractal) system. A schematic of a fractured reservoir is shown in Fig. 1. We assume that the fractured reservoir consists of a complex distribution of natural fractures, which is characterized through fractal geometry. There is natural flow in the horizontal (X-axis) direction, and the main fluid trend is flowing along fractures. The reservoir is surrounded by rock masses of lower permeability. An understanding emerged of the importance of general non-locality in upscaled transport in heterogeneous aquifer material. The non-locality arises when the underlying velocity field is uncertain and correlation scales are significantly large relative to the scale of observation (Zhang et al., 2009). On the basis of the above assumptions, the governing equation of mass transport in a fractured reservoir is derived as follows:

$$\phi\frac{\partial c}{\partial t} + a\frac{\partial^\gamma c}{\partial t^\gamma} + a'\frac{\partial^\beta c}{\partial t^\beta} = -\frac{\partial(\phi J)}{\partial x} - v\frac{\partial c}{\partial x} \tag{2}$$

where t and x are time and distance, respectively; c and J are the mean concentration and the mean diffusive mass flux in the fractured reservoir, respectively; ϕ the porosity; a and a' the retardation factors, which are related to dispersion process into secondary branched fractures and diffusion into surrounding rocks, respectively; v the mean velocity, at which the flow of solutions occurs only along fractures; and β $(0.5<\beta<1)$ and γ $(0.5\leq\gamma\leq1)$ are the order of fractional temporal derivatives. One attempt to incorporate spatial non-locality in a tractable form assumed a power-law kernel, which forms the definition of a fractional-order dispersion term, as follows:

$$J = -D\left(p\frac{\partial^\alpha c}{\partial x^\alpha} + (1-p)\frac{\partial^\alpha c}{\partial(-x)^\alpha}\right) \tag{3}$$

where D is the dispersion coefficient, p $(0 \le p \le 1)$ the skew parameter that controls the bias of the dispersion (Huang et al., 2006), and α $(0 < \alpha \le 1)$ is the order of fractional spatial derivative. The first and second terms on the right side are written with the left-handed and right-handed fractional derivatives, respectively. The left-handed fractional derivative of c at a point x depends on all function values to the left of point x, i.e., this derivative is a weighted average of such function values. Similarly, the right-handed fractional derivative of c at a point x depends on all function values to the right of this point (Deng et al., 2004; Meerschaert and Tadjeran, 2006; Huang et al., 2006).

To normalize Eqs. (2) and (3), the non-dimensional variables are defined as follows:

$$X = \frac{x}{l}; \quad C = \frac{c_2}{c_m}; \quad \tau = \frac{t}{t_m}; \quad Pe = \frac{l^{1+\alpha}}{t_m D}; \quad v = \phi \frac{l}{t_m};$$
$$b_1 = \frac{a_1}{\phi t^{\beta-1}}; \quad b_3 = \frac{a_3}{\phi t^{\gamma-1}} \tag{4}$$

Substituting Eq. (3) into Eq. (2), the normalized equation can be written as follows:

$$\frac{\partial C}{\partial \tau} + b\frac{\partial^\gamma C}{\partial \tau^\gamma} + b'\frac{\partial^\beta C}{\partial \tau^\beta} = \frac{1}{Pe}\frac{\partial}{\partial X}\left(p\frac{\partial^\alpha C}{\partial X^\alpha} + (1-p)\frac{\partial^\alpha C}{\partial(-X)^\alpha}\right) - \frac{\partial C}{\partial X} \tag{5}$$

where C, T, and X are concentration, time and distance, which are normalized with respect to each representative value. The representative concentration is the injected concentration at the inlet point. The velocity in Eq. (2) makes a correlation between the representative time and distance. b and b' are the retardation coefficient and Pe is Péclet number. Here, the first term on the left side of Eq. (5) is the accumulation term, and the second term on the left side of Eq. (5) models the retardation process associated with dispersion into secondary branched fractures. The third term on the left side is the process of vertical dispersion into surrounding rock masses. The first and second terms on the right side express dispersion within the fractured reservoir, and the third term is the advection term.

2.2. Discretization of the governing equation

Fomin et al. (2011) derived the analytical solution of Eq. (5), which takes no account of the dispersion term. In contrast, since the dispersion term with space fractional derivative expresses dispersion behaviors in fractal heterogeneous media, it is likely to characterize fractal geometry within the fractured reservoir. Hence, we develop a finite discrete method to derive a numerical solution to Eq. (5) including a fractional derivative in space. The fractional derivative defined by the Riemann–Liouville definition could lead to unphysical results when applied to simulate solute movement within a bounded domain (Zhang et al., 2007). To overcome this problem, a fractional dispersive flux with the Caputo derivatives is used in this study. The Caputo definition is

$$\frac{d^\alpha f}{dt^\alpha} = \begin{cases} \dfrac{1}{\Gamma(m-\alpha)}\displaystyle\int_0^t (t-\tau)^{-\alpha-1+m} f(\tau)^{(m)}\, d\tau; & m-1 < \alpha < m \\ \dfrac{d^m f}{dt^m} f(t); & \alpha = m \end{cases} \tag{6}$$

The boundaries are prescribed at the inlet ($X = 0$) and the outlet ($X = L$). The implicit scheme has first-order accuracy of the differences in time, and of upwind difference in dispersion term and in advection term.

Eq. (5) can be represented in discrete numerical form as:

$$\frac{C_i^{n+1} - C_i^n}{\Delta T} + \frac{b}{\Delta T^\gamma}\sum_{k=0}^{n} w_k^\gamma C_i^{n-k+1} + \frac{b'}{\Delta T^\beta}\sum_{k=0}^{n} w_k^\beta C_i^{n-k+1}$$
$$= \frac{1}{Pe}\frac{\vartheta_i^{n+1} - \vartheta_{i-1}^{n+1}}{\Delta X} - \frac{C_i^{n+1} - C_{i-1}^{n+1}}{\Delta X} \tag{7}$$

where $w_0^\gamma = 0$, $w_k^\gamma = (-1)^k \frac{(\gamma+1)\gamma(\gamma-1)\cdots(\gamma-k+1)}{k!}$. ΔX is the grid size, and ΔT is the integration time. We use X_i to represent the coordinate of the ith grid and let C_i^n and J_i^n be the concentration and mass flux of the ith grid at nth time step, respectively. $\vartheta_i^n = p\frac{\partial^\alpha C}{\partial X^\alpha} + (1-p)\frac{\partial^\alpha C}{\partial(-X)^\alpha}\Big|_i^n$. Mass flux ϑ_i^n and ϑ_{i-1}^n can be represented via Eqs. (14) and (15), from Zhang et al. (2007)

$$\vartheta_i^n = \frac{1}{\Gamma(2-\alpha)\Delta X^\alpha} \times \left(\sum_{j=0}^{i} p\psi_j(C_{i-j+1} - C_{i-j}) + \sum_{j=0}^{N-i+1}(1-p)\psi_j(C_{i+j+1} - C_{i+j})\right) \tag{8}$$

$$\vartheta_{i-1}^n = \frac{1}{\Gamma(2-\alpha)\Delta X^\alpha} \times \left(\sum_{j=0}^{i-1} p\psi_j(C_{i-j} - C_{i-j-1}) + \sum_{j=0}^{N-i}(1-p)\psi_j(C_{i+j} - C_{i+j-1})\right) \tag{9}$$

where $\psi_j = (j+1)^{1-\gamma} - j^{1-\gamma}$.

We focus on prescribed-flux boundary commonly encountered in hydrology: a prescribed flux at the inlet $x = 0$ and a free drainage at the outlet $x = L$, which can be expressed as follows:

$$C - \frac{1}{Pe}\left(p\frac{\partial^\alpha C}{\partial X^\alpha} + (1-p)\frac{\partial^\alpha C}{\partial(-X)^\alpha}\right)\Bigg|_{x=0} = C_{in} \tag{10}$$

$$\left(p\frac{\partial^\alpha C}{\partial X^\alpha} + (1-p)\frac{\partial^\alpha C}{\partial(-X)^\alpha}\right)\Bigg|_{x=L} = 0 \tag{11}$$

2.3. Verification against analytical solutions

The numerical scheme to obtain the solutions of Eq. (5) was verified against the analytical solutions. Fomin et al. (2011) derived the analytical solution of the fADE, in which the first and second terms on the right side were negligible. Calculating the Laplace transform of Eq. (5) gives

$$C(T, X) = \frac{\partial}{\partial T}\int_0^T C_{in}(T-\xi)\chi(\xi - X)\psi(\xi - X, X)\, d\xi \tag{12}$$

where χ is a unit step function, and ψ is defined as:

$$\psi(T, X) = 1 - \frac{1}{\pi}\int_0^\infty \exp[-\xi T - X(b\xi^\gamma \cos(\pi\gamma) + \xi^\beta \cos(\pi\beta))] \times \sin[X(b\xi^\gamma \sin(\pi\gamma) + \xi^\beta \sin(\pi\beta))] \tag{13}$$

Comparisons of numerical solution of Eq. (5) with analytical solutions of Eq. (12), where tracers are injected as steps and as pulses at the inlet boundary, are shown in Fig. 2(a) and (b), respectively. ΔX and ΔT are set to 0.1. The injected time T_{in} is 100.0, and the maximum length L is 100.0. Since the calculated solutions were rarely different from the solutions using more coarse mesh sizes,

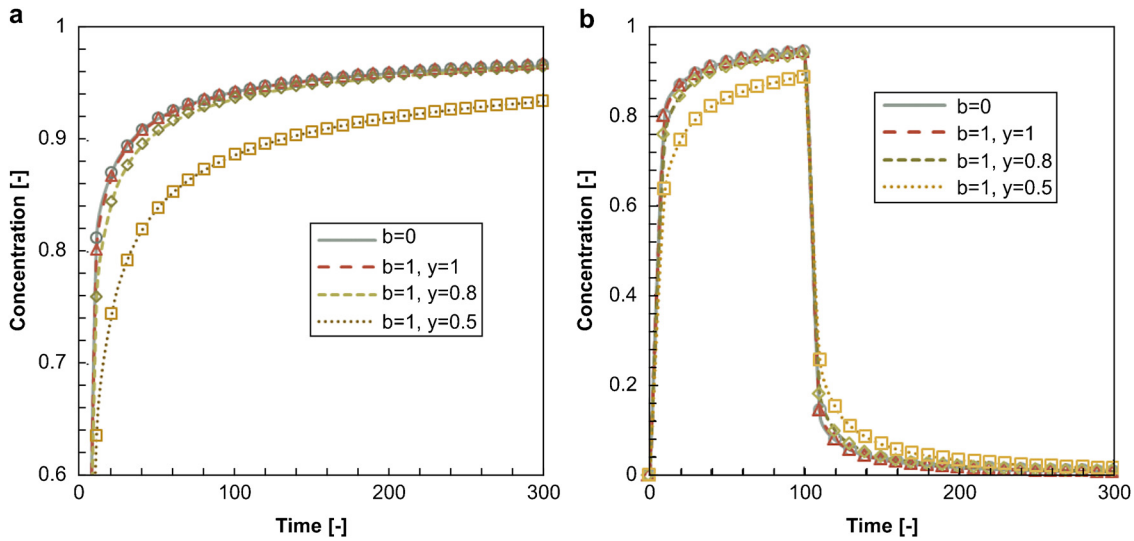

Fig. 2. Analytical and numerical solutions of the fADE at $X = 1$ for $b = 1$, $\beta = 0.5$, and $Pe = \infty$. (a) Tracers are injected as steps for $C_{in} = 1$, and (b) as pulse for $C_{in} = 1$ and $T_{in} = 1$.

the impacts of spatial and temporal step-size on the numerical dispersion can be eliminated. The results showed very good agreement with the analytical solutions.

3. Remarks on simulation

To validate a tracer analysis method based on the fADE, numerical simulation was conducted to characterize tracer responses and evaluate the prediction of mass transport by the fADE. We use FRACSIM-3D to obtain tracer responses in a fractured reservoir, which is based on a fracture network model considering fractal geometry (Watanabe and Takahashi, 1995; Willis-Richards et al., 1996). Jing et al. (2000) showed that tracer responses calculated by FRACSIM-3D had similar characteristics to field data; hence, we consider that the numerical code of FRACSIM-3D is effective to provide tracer data.

The numerical algorithm in FRACSIM-3D, based on a fracture network model, is schematically shown in Fig. 3. The calculation domain and calculation conditions are shown in Fig. 4 and listed in Table 1, respectively. Although Eq. (5) accounts for the effect of diffusion into surrounding rocks, this study assumes that the permeability of surrounding rocks is negligible, and that fluid only flows within the reservoir.

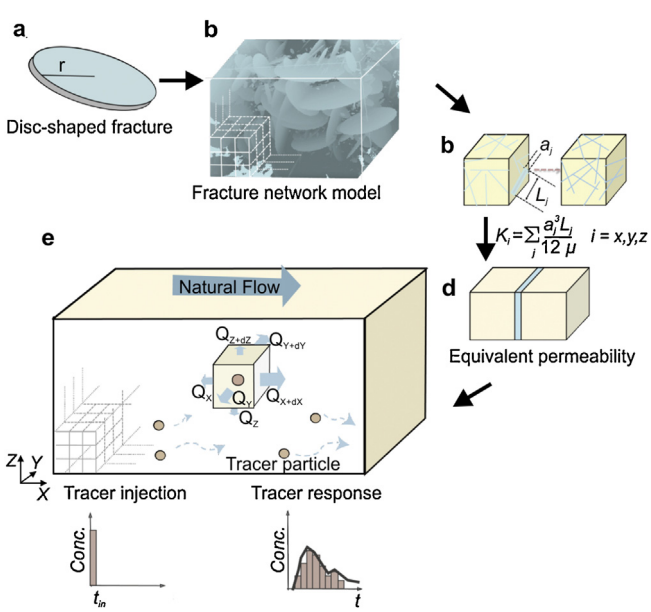

Fig. 3. Concept of tracer response analysis based on the fractured reservoir model.

A distributed fracture is disk-shaped with several lengths (Fig. 3(a)). The fracture radius, r, is generated based on the fractal geometry, which was demonstrated to be capable of mathematically representing the geometry of natural fractures (Watanabe and Takahashi, 1995). Fractures are generated until the fracture density reaches the determined level with power-law fracture length distribution. The number of fractures, N, is then given by:

$$N = C_f[r_{\min}^{-D_f} - r_{\max}^{-D_f}] \tag{14}$$

where C is the fracture density parameter and D_f is the fractal dimension; $r_{\min}$ and $r_{\max}$ are the specified radii of the smallest and largest fractures in the model, respectively. The locations and orientations of individual fractures are assumed to be random. Furthermore, it is assumed that the aperture of a circular fracture, a_i, is proportional to its radius.

In the 3D model, flow analyses are conducted on a square grid, and the network model is solved by converting the network to an equivalent continuum mesh, as illustrated in Fig. 3(b). We set up calculations in the x, y, and z directions in a 540 m × 250 m × 250 m domain on a 540 × 250 × 250 grid. According to the cubic law, the distribution of effective permeability for each block surface, K_i, can

Table 1
Parameters used for the simulation.

Parameters	Value
Calculation domain [m]	540 × 250 × 250
Element size [m]	1 × 1 × 1
Fractal dimension	2
Fracture radius, r [m]	2–60
Fracture aperture [m]	$1.0 \times 10^{-4} \times r$
Injection pressure [Pa]	1.001×10^5
Production pressure [Pa]	1.0×10^5
Matrix permeability [m^2]	0
Viscosity of water [Pa s]	1.826×10^{-4}
Number of tracer particles	1.0×10^4

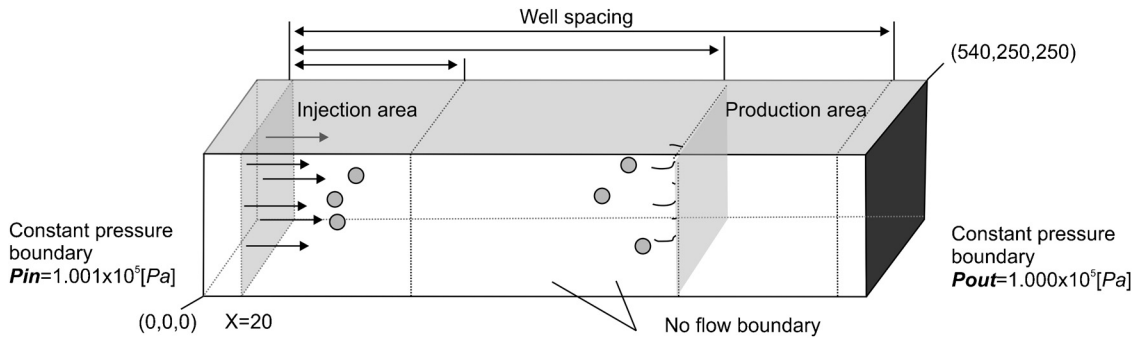

Fig. 4. Schematic of computation domain.

be calculated by the sum of products from each of the penetrating fractures, as follows (Fig. 3(c)):

$$K_i = \sum_{j=1}^{N} \frac{a_j^3 L_j}{12\mu}, \quad i = x, y, z \tag{15}$$

where N is the total number of penetrating fractures, a_i the fracture aperture, L_i the fracture intersection length, and μ is the viscosity of water. Effective flow rates given for each block surface are calculated on the basis of Darcy's law. We assume one-dimensional flow within the reservoir and use a constant pressure at inlet and outlet boundaries. Inlet boundary pressure was 1.001×10^5 Pa and outlet boundary pressure was 1.0×10^5 Pa. Other boundaries are no-flow boundaries. Horizontal pressure gradient in the x direction within the reservoir is approximately constant. We assume a flow system of a natural hydraulic state before production operation, which means that pressure change associated with production has no effect on pressure distribution.

A total of 10,000 tracer particles are released as a pulse in a vertical plane $X = 20$ (see Fig. 3(e)). The direction of travel for each tracer is determined by probabilities based on the magnitude of flow rate on each element surface. Each time is calculated during which a tracer migrates at individual elements, and we can now calculate the cumulative travel time for individual tracer particles between the injection area and production area. In this study, the temporal distribution of the tracer particles that arrive at the production area, is used as tracer response curves. All tracer trajectories can be investigated, and the numerical dispersion with respect to tracer concentration has no impact on the tracer responses.

4. Results and discussion

A flow simulation was performed to investigate the effect of fracture density on tracer response behavior. Tracer data at fracture densities of 6.4 [1/m] and 0.6 [1/m] are shown in Fig. 5. The fracture density represents the mean number of fracture traces per unit length [1/m]. Note that well spacing is 50 m. The tracer responses were normalized by representative physical variables. That is, the normalized distance X is the length divided by well spacing (here 50 m). The normalized time t is the present time-interval divided by the average time that tracers travel between the well spacing. As mentioned in previous session, concentration C is normalized using injected concentration. In the case where fluid flow within a reservoir is subject to not only advection but also dispersion, average travel time can be calculated as (Käss et al., 1998):

$$T_{\text{effective}} = \frac{T_{\text{peak}} + T_{\text{median}}}{2} \tag{16}$$

where T_{peak} is the peak time at observation point and T_{median} is the time at which 50% of the recovered tracer mass passed the observation borehole.

A concentration profile at fracture density of 0.6 [1/m] demonstrates a long tailing, as shown in Fig. 5. The tailing of tracers is a feature of anomalous dispersion observed in geothermal fields and laboratory experiments. In order to investigate the heterogeneity of fracture distribution for different fracture densities, frequency distributions of permeability were calculated for each element. The permeability is the average equivalent permeability calculated on each element surface. The frequency distribution of permeability is shown in Fig. 6. The permeability distribution at fracture density of 0.6 [1/m] does not exhibit symmetrical behavior, unlike the results for fracture density of 6.4 [1/m]. In addition, 40% of elements

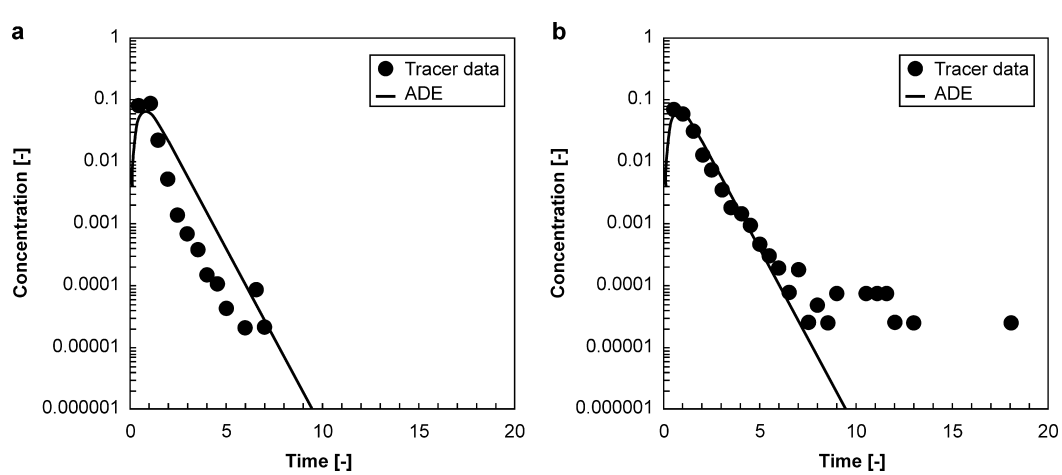

Fig. 5. Effects of fracture density on tracer responses at fracture density of (a) 6.4 [1/m] and (b) 0.6 [1/m]. The solid lines are fitting curves by the ADE.

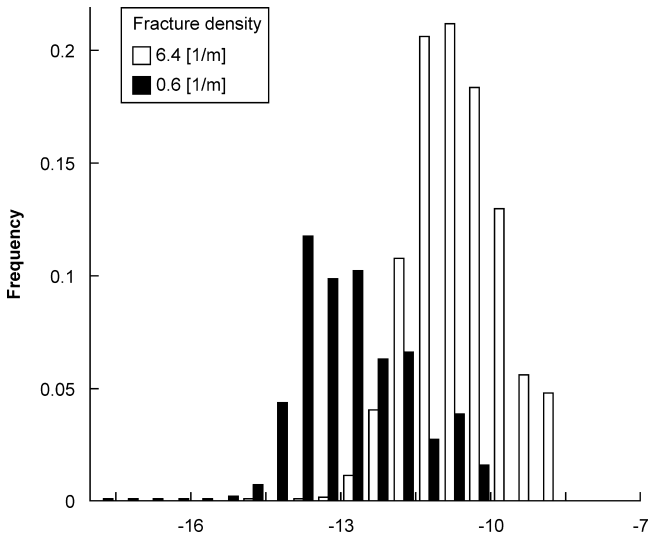

Fig. 6. Histogram of distributed permeability in fracture network model.

are given zero permeability because the element does not cross any fractures in the case of low fracture density. It is evident that fractures are distributed heterogeneously, and that the permeability values vary widely according to location. Therefore, a fracture network model that distributes the same long fractures without consideration of fractal geometries provides less variability of permeability distribution, and the tracer response does not exhibit a long tail. Hence, the long tail produced by FRACSIM-3D is attributed to the heterogeneous permeability based on fractal representation of fracture lengths.

Fig. 7(a) shows tracer data calculated by FRACSIM-3D at fracture density of 1.5 [1/m] and well spacing of 50 m. Models of the ADE and the fADE were fitted for the response curve. In this study, we assume that the permeability of surrounding rocks is relatively low, and that flow occurs only within the reservoir. Hence, the effect of diffusion into surrounding rocks, expressed by the third term on the left side in Eq. (5), can be regarded as negligible. Furthermore, in the case where fluid flow within a reservoir is subject to preferential flow paths due to fracture network, it is known that the skewness parameter, p, is less than 1/2. In some studies, p was set to zero (i.e., Zhang et al., 2007). The fracture network model used in this study includes preferential flow paths with relatively strong connectivity between fractures. In order to achieve a development of the fADE, we simply set $p = 0$. Consequently, the fADE constitutive parameters obtained from curve-fitting are α, γ, b, and Pe. Note that the case where $\alpha = 1$ and $\gamma = 1$ in Eq. (5) corresponds to

Table 2
RMSE (root mean square error) as indicator of prediction performance.

Well spacing [m]	RMSE	
	ADE	fADE
50 (fitting)	3.63	0.14
250	2.16	0.20
450	1.80	0.20

the ADE model. The optimization program ADS (Vandenplaats and Sugimoto, 1986) was used, which is based on the conjugated gradient method. The objective function is set to the root mean square error (RMSE) between tracer data and numerical solutions of both of the models. RMSE is

$$\mathrm{RMSE} = \sqrt{\frac{1}{N}\sum_{i=1}^{N}(\log C_i^{\mathrm{fADE}} - \log C_i^{\mathrm{tracer}})^2} \tag{17}$$

and is calculated by the logarithm of the concentrations in order to provide adequate comparison with respect to long-time tailing as well as peak concentration; N is the number of data, C_i^{fADE} the concentration calculated by the fADE, and C_i^{tracer} the concentration obtained by FRACSIM-3D.

The optimization of the constitutive parameters gives $b = 0.08$ and $Pe = 4.29$ in the ADE; and $\alpha = 0.1$, $\gamma = 1.0$, $b = 0.65$, and $Pe = 1.63$ in the fADE. The tracer results at well spacing of 250 m and 450 m exhibit long tails, as shown in Fig. 7(b) and (c). Here, the ADE gives a symmetrical distribution and cannot describe the long tails. On the other hand, the fADE is in good agreement with the tracer response even including long tails. RMSE is summarized in Table 2. As a result from optimization of the fADE constitutive parameters, the temporal fractional derivative, γ is determined as $\gamma = 1.0$. It is reasonable to suppose that the description of the tracer behavior does not require the temporal fractional derivative here. Namely, the long tails in the tracer response can be characterized by using the spatial fractional derivative in Eq. (5).

The tracer responses at wide well-spacing were predicted via the above-optimized parameters in both the fADE and ADE, shown in Fig. 6. Table 2 summarizes the RMSE to describe average model-performance error for each well-spacing scenario. With consideration for changes in peak concentration at different well spacing, the normalized concentration is the calculated concentration divided by the peak concentration for each well spacing. As shown in Fig. 6, the peak concentrations retard and decline with greater well spacing. In addition, each tracer response exhibits significant late tails. The ADE model can predict the peak concentration of tracers and the peak time, but cannot characterize long tails. In contrast, the fADE model can predict peak concentration,

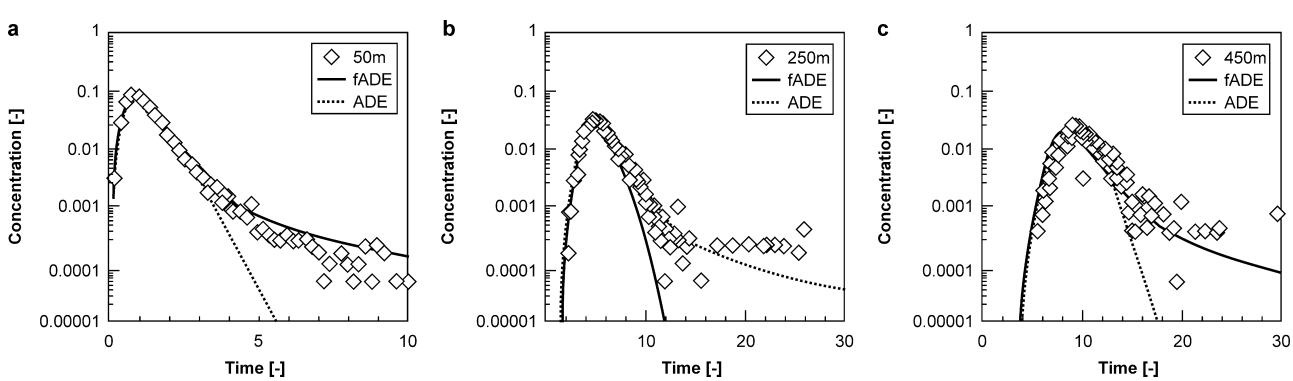

Fig. 7. Breakthrough curves for one-dimensional flow. Rectangles are simulation results by FRACSIM-3D at well spacings of (a) 50 m, (b) 250 m, and (c) 450 m. Solid lines are (a) best fit with the fADE; (b) and (c) are predicted results of the fADE. Dashed lines are (a) best fit with the ADE; (b) and (c) are predicted results of the ADE.

peak time, and the feature of long tails. This prediction suggests that the fADE constitutive parameters, which are determined using data from close and distant well-spacings, are the same. It would be more appropriate to state that the constitutive parameters of the fADE can characterize the entire field without dependence on well spacing.

In order to optimize injection strategies in geothermal fields, evaluation is required of heat transfer, pressure propagation, and mass transport. As an analogy between mass transport and heat transfer, tracer response provides the possibility of predicting thermal breakthrough due to injection (Shook, 1999). By expansion of the fADE model in combination with thermal and pressure behaviors, it is likely to enable a new approach to designing reservoirs that are composed of complex fracture networks. Further modeling of heat transfer and/or pressure propagation based on the fADE model through fractured media, taking into account into the fractal of the fracture length, may be warranted.

The fADE can predict anomalous behaviors of tracer responses using few parameters. Numerical simulations (e.g., discrete fracture network model, MINC model) and other mathematical models (e.g., flow-channeling model, fracture-matrix model) require many input parameters in order to represent complex fractured reservoirs. In particular, limited and uncertain measurement data at the beginning of any field development are incapable of providing unique model-constitutive parameters. In such cases, fADE, which summarizes complexity based on fractal geometry, is expected to quickly and efficiently analyze mass transport in a fractured reservoir.

5. Concluding remarks

In this paper, we have presented a numerical method for solving a fractional advection-dispersion equation to model mass transport in fractured reservoirs. Comparison with the analytical solutions confirms the reliability of the finite difference algorithms.

A 3D simulation code for flow analysis (FRACSIM-3D) is utilized to produce numerical data for tracer responses. Analysis of the effects of fracture density on tracer behaviors shows that the tracer response curve obtained in heterogeneous fracture distribution at low fracture density showed highly anomalous behaviors such as a long tail. While the advection-dispersion equation (ADE) differs from the tracer response curve exhibiting a long tail, the fADE solution incorporating a space fractional derivative showed reasonable agreement with the tracer data. The long tail in the tracer response calculated by FRACSIM-3D is attributable to a heterogeneous permeability distribution based on the fractal of fracture length. The fitting parameters at well spacing of 50 m were used to make predictions at spacings of 250 m and 450 m. This study demonstrates that the fADE can predict tracer responses over different distances in a fractured reservoir. In order to optimize injection strategies in geothermal fields, further fADE modeling may be warranted of heat transfer and/or pressure propagation through fractured media, taking into account the fractal of fracture lengths. The fADE makes it possible to quickly and efficiently analyze mass transport in a fractured reservoir.

Acknowledgements

This work was supported by a Grant-in-Aid for Japanese Society for the Promotion of Science Fellows (no. 23-3250).

References

Axelsson, G., Stefánsson, V., Björnsson, G., Liu, J., 2005. Sustainable management of geothermal resources and utilization for 100–300 years. In: Proceedings of the 2005 World Geothermal Congress, Antalya, Turkey, 24–29 April, Paper 507, 8 pp.

Barenblatt, G.I., Zheltov, I.P., Kochina, I.N., 1960. Basic concepts in the theory of seepage of homogeneous liquids in fissured rocks. J. Appl. Math. Mech. 24, 1286–1303.

Bear, J., 1972. Dynamics of Fluids in Porous Media. American Elsevier, New York.

Benson, D.A., Wheatcraft, S.W., Meerschaert, M.M., 2000a. The fractional-order governing equation of Lévy motion. Water Resour. Res. 36 (6), 1413–1423.

Benson, D.A., Wheatcraft, S.W., Meerschaert, M.M., 2000b. Application of a fractional advection-dispersion equation. Water Resour. Res. 36 (6), 1403–1412.

Bullivant, D.P., O'Sullivan, M.J., 1989. Matching a field tracer test with some simple models. Water Resour. Res. 25 (8), 1879–1891.

Coats, K.H., Smith, B.D., 1964. Dead-end pore volume and dispersion in porous media. SPE J. 4 (1), 73–84.

Deng, Z.Q., Singh, V.P., Bengtsson, L., 2004. Numerical solution of fractional advection-dispersion equation. J. Hydraul. Eng. 130, 422–431.

Fomin, S.A., Chugunov, V.A., Hashida, T., 2011. Non-Fickian mass transport in fractured porous media. Adv. Water Resour. 34 (2), 205–214.

Gerke, H.H., van Genuchten, M.T., 1993. A dual-porosity model for simulating the preferential movement of water and solutes in structured porous media. Water Resour. Res. 29 (2), 305–319.

Gringarten, A.C., Sauty, J.P., 1975. A theoretical study of heat extraction from aquifers with uniform regional flow. J. Geophys. Res. 80 (35), 4956–4962.

Gringarten, A.C., Witherspoon, P.A., Ohnishi, Y., 1975. Theory of heat extraction from fractured hot dry rock. J. Geophy. Res. 80 (8), 1120–1124.

Hatano, Y., Hatano, N., 1998. Dispersive transport of ions in column experiments: an explanation of long-tailed profiles. Water Resour. Res. 34 (5), 1027–1033.

Horne, R.N., 1985. Reservoir engineering aspects of reinjection. Geothermics 14 (2–3), 449–457.

Huang, G., Huang, Q., Zhan, H., 2006. Evidence of one-dimensional scale-dependent fractional advection-dispersion. J. Contam. Hydrol. 85 (1), 53–71.

Jing, Z., Willis-Richards, J., Watanabe, K., Hashida, T., 2000. A three-dimensional stochastic rock mechanics model of engineered geothermal systems in fractured crystalline rock. J. Geophys. Res. 105 (B10), 23663–23679.

Juliusson, E., Horne, R.N., 2013. Optimization of injection scheduling in fractured geothermal reservoirs. Geothermics 48, 80–92.

Kaya, E., Zarrouk, S.J., O'Sullivan, M.J., 2011. Reinjection in geothermal fields: a review of worldwide experience. Renew. Sustain. Energy Rev. 15 (1), 47–68.

Käss, W., Behrens, H., Hötzl, H., 1998. Tracing Technique in Geohydrology. Balkema, Rotterdam.

Kazemi, H., 1969. Pressure transient analysis of naturally fractured reservoirs with uniform fracture distribution. SPE J. 9 (4), 451–462.

Kocabas, I., 2005. Geothermal reservoir characterization via thermal injection backflow and interwell tracer testing. Geothermics 34, 27–46.

Lauwerier, H.A., 1955. The transport of heat in an oil layer caused by the injection of hot fluid. Appl. Sci. Res. 5, 145–150.

Long, J.C.S., Witherspoon, P.A., 1985. The relationship of the degree of interconnection to permeability in fracture networks. J. Geophys. Res. 90 (B4), 3087–3098.

Lovekin, J., Horne, R.N., 1989. Optimization of injection scheduling in geothermal fields. In: Proceedings of the Geothermal Program Review VII, pp. 45–52.

Meerschaert, M.M., Tadjeran, C., 2006. Finite difference approximations for two-sided space-fractional partial differential equations. Appl. Numer. Math. 56, 80–90.

Moreno, L., Neretnieks, I., Eriksen, T., 1985. Analysis of some laboratory tracer runs in natural fissures. Water Resour. Res. 21 (7), 951–958.

Neretnieks, I., Eriksen, T., Tähtinen, P., 1982. Tracer movement in a single fissure in granitic rock: some experimental results and their interpretation. Water Resour. Res. 4 (18), 849–858.

Neretnieks, I., 1983. A note on fracture flow dispersion mechanisms in the ground. Water Resour. Res. 19 (2), 364–370.

Neuman, S.P., 2005. Trends, prospects and challenges in quantifying flow and transport through fractured rocks. Hydrogeol. J. 13, 124–147.

Niibori, Y., Ogura, H., Chida, T., 1995. Identification of geothermal reservoir structure analyzing tracer responses using the two-fractured-layer model. Geothermics 24 (1), 49–60.

Pruess, K., Bodvarsson, G., 1984. Thermal effects of reinjection in geothermal reservoirs with major vertical fractures. J. Petrol. Technol. 36, 1567–1578.

Pruess, K., Narasimhan, T.N., 1985. A practical method for modeling fluid and heat flow in fractured porous media. Soc. Pet. Eng. J. 25, 14–26.

Pruess, K., 2002. Numerical simulation of 'multiphase tracer transport in Fractured Geothermal Reservoirs. Geothermics 31 (4), 475–499.

Rose, P.E., Mella, M., Kasteler, C., Johnson, S.D., 2004. The estimation of reservoir pore data from tracer data. In: Proceedings of 29th Workshop on Geothermal Reservoir Engineering, Stanford University, SGP-TR-175.

Schumer, R., Benson, D.A., Meerschaert, M.M., Baeumer, B., 2003. Fractal mobile/immobile solute transport. Water Resour. Res. 39 (10), 1296, http://dx.doi.org/10.1029/2003WR002141.

Suzuki, A., Makita, H., Niibori, Y., Fomin, S.A., Chugunov, V.A., Hashida, T., 2012. Characterization of tracer responses using fractional derivative-based mathematical model and its application to prediction of mass transport in fractured reservoirs. GRC Trans. 36, 1391–1396.

Shook, G.M., 1999. Prediction of thermal breakthrough from tracer tests. In: Proceedings of 24th Stanford Workshop on Geothermal Reservoir Engineering, SGP-TR-162.

Shook, G.M., 2001. Predicting thermal breakthrough in heterogeneous media from tracer tests. Geothermics 30 (6), 573–589.

Stefansson, V., 1997. Geothermal reinjection experience. Geothermics 26 (1), 99–139.
Tsang, Y.W., Tsang, C.F., 1987. Channel model of flow through fractured media. Water Resour. Res. 23 (3), 467–479.
Vandenplaats, G.N., Sugimoto, H., 1986. A general-purpose optimization program for engineering design. Int. J. Comput. Struct. 24, 13–21.
Watanabe, K., Takahashi, H., 1995. Fractal geometry characterization of geothermal reservoir fracture networks. J. Geophys. Res. 100 (B1), 521–528.
Warren, J.E., Root, P.J., 1963. The behavior of naturally fractured reservoirs. SPE J. 3 (3), 245–255.
Willis-Richards, J., Watanabe, K., Takahashi, H., 1996. Progress toward a stochastic rock mechanics model of engineered geothermal systems. J. Geophys. Res. 101 (B8), 17481–17496.
Wu, X., Pope, G.A., Shook, G.M., 2008. Prediction of enthalpy production from fractured geothermal reservoirs using partitioning tracers. Int. J. Heat Mass Transfer 51 (5–6), 1453–1466.
Zhang, X., Lv, M., Crawford, J.W., Young, I.M., 2007. The impact of boundary on the fractional advection-dispersion equation for solute transport in soil: defining the fractional dispersive flux with the Caputo derivatives. Adv. Water Resour. 30 (5), 1205–1217.
Zhang, Y., Benson, D.A., Reeves, D.M., 2009. Time and space nonlocalities underlying fractional-derivative models: distinction and literature review of field applications. Adv. Water Resour. 32 (4), 561–581.
Zimmerman, R.W., Bodvarsson, G.S., 1996. Effective transmissivity of two-dimensional fracture networks. Int. J. Rock Mech. Mining Sci. Geomech. Abstr. 33 (4), 433–488.